REPORT DOCUMENTATION PAGE

Form Approved
OMB No. 0704-0188

1. REPORT DATE *(DD-MM-YYYY)*	2. REPORT TYPE	3. DATES COVERED *(From - To)*
31/08/2005	Status Report	1/02/2005 - 31/07/2005

4. TITLE AND SUBTITLE
Fully integrated, multiport, planar-waveguide spectral comparators and multiplexers based on lithographic holography

5a. CONTRACT NUMBER
DASG60-03-C-0088

5b. GRANT NUMBER

5c. PROGRAM ELEMENT NUMBER

6. AUTHOR(S)
Dr. Thomas Mossberg, Principal Investigator

Report prepared by:
Dr. Christoph Greiner

5d. PROJECT NUMBER

5e. TASK NUMBER
0002

5f. WORK UNIT NUMBER

7. PERFORMING ORGANIZATION NAME(S) AND ADDRESS(ES)
LightSmyth Technologies, Inc.
860 W. Park Street, Suite 250
Eugene, OR 97401
(541) 431-0026

8. PERFORMING ORGANIZATION REPORT NUMBER
LST-DASG60-0002

9. SPONSORING/MONITORING AGENCY NAME(S) AND ADDRESS(ES)
U.S. Army Space & Missile Defense Command
SMDC-CM-A, James
Patricia James (256) 955-4167
P. O. Box 1500
Huntsville, AL 35807-3801

10. SPONSOR/MONITOR'S ACRONYM(S)
SMDC

11. SPONSOR/MONITOR'S REPORT NUMBER(S)

12. DISTRIBUTION/AVAILABILITY STATEMENT
Approved for public release; distribution unlimited

13. SUPPLEMENTARY NOTES

14. ABSTRACT
Several multiplexer layouts based on holographic Brag reflectors were designed and fabricated in a preliminary device wafer. Fabrication results constitute, for the first time, the successful application of HBRs to wavelength division multiplexing. Measured device performance indicates that the photolithographic fabrication process has reduced multiplexer designs to practice essentially perfectly. Device apodization and engineering of multiplexer spectral transfer functions based on partial writing and offsetting of diffractive contours is shown to function with high fidelity. A compact-footprint multiplexer based on overlay of several HBRs on the same area was demonstrated. A novel approach to the control and mitigation of waveguide birefringence has been devised successfully.

15. SUBJECT TERMS
Integrated holographics; holographic Bragg reflectors; deep ultraviolet lithography; dense wavelength division multiplexers; spectral comparators

16. SECURITY CLASSIFICATION OF:			17. LIMITATION OF ABSTRACT	18. NUMBER OF PAGES	19a. NAME OF RESPONSIBLE PERSON
a. REPORT	b. ABSTRACT	c. THIS PAGE			Sarah Laszlo
U	U	U	Unclassified	17	19b. TELEPHONE NUMBER *(Include area code)* (541) 431-0026

SBIR Phase III Status Report
Contract Number DASG60-03-C-0088
Title Page

Project Name

Fully integrated, Multiport, Planar-waveguide, Spectral Comparators and Multiplexers based on Lithographic Holography

Reporting Period

CDRL Data Item A002, Status Report III, February 1, 2005 - July 31, 2005

Contractor Name and Address

LightSmyth Technologies, Inc.
860 W. Park, Suite 250
Eugene, OR 97401

Purchase Request Number

SM4A863200-01B; ACRN AB
W31RPD5041CNQ2-01; ACRN AC

Principal Investigator

Dr. Thomas Mossberg
(541) 431-0027
twmoss@lightsmyth.com

Report prepared by

Dr. Christoph Greiner
(541) 431-0029
cgreiner@lightsmyth.com

1. Summary

1.1. General Background and Review

The present SBIR effort relates to the development of *integrated holographics* - a disruptive new photonics technology – and its application to optical spectral comparators and dense wavelength division multiplexers. The engines or functional building blocks of *integrated holographics* relevant to this application space are planar two-dimensional (2D) holographic Bragg reflectors (HBRs). *Integrated holographics* is a highly versatile photonics technology that has many other applications besides those pursued in the present work. These include optical code division multiplexing (O-CDMA), RF photonics, remote sensing and homeland security related applications as well as correlation-based optical temporal waveform recognition, important for address label recognition on optical packet-switched networks. Integrated holographics and HBR-based devices are projected to provide substantially superior performance compared to alternative competing technologies in these areas.

2D HBRs are volume-holographic slab-waveguide-based etched refractive-index structures that provide powerful dual signal processing functionality since they both spectrally filter and spatially route signals in a single element. From a fundamental view, 2D HBRs facilitate a novel form of photonic signal processing and transport that is based on the principles of holography and allows for free-space-like signal propagation, albeit in the fully integrated planar lightwave circuit (PLC) environment. This concept is fundamentally different from typical electronics-style channel-waveguide interconnections encountered in traditional PLC-based devices and eliminates the need for associated and constraining space requirements. Holographic mapping using planar HBRs opens the door to unique integrated photonic circuits of ultra-compact footprint, called distributed photonic circuits, wherein signals can propagate and overlap freely as they are imaged from element to element.

The present effort aims to explore the fabrication of HBR-based dense wavelength division multiplexers and multiport spectral comparators by *lithographic holography* – a fabrication approach pioneered by LightSmyth Technologies. The use of modern deep ultraviolet lithographic methods and novel planar waveguide materials to fully harness the processing powers of computer-generated holographic design comprises a paradigm shift in the fabrication of photonic devices. Only recently has lithographic resolution evolved to the fineness level needed to support general holographic devices. For the first time, the full signal processing power of holography is available without the constraints of optical interferometric fabrication and unstable photosensitive recording materials.

1.2. Objectives of Present 6-Month Effort

Our technical objectives in this Phase II proposal are to demonstrate the detailed design, fabrication, and operational properties of planar HBR-based dense wavelength-division multiplexing (DWDM) optical multiplexers. Within the 24-month effort we will proceed through multiple design/fab/test cycles ramping the performance factors as the cycles progress. At the end of the proposed program, clear demonstration of high level function will be available in fully integrated chip form. A detailed task schedule for the effort is given in section 2.2.a. We briefly review here the objectives pertinent to the present reporting period.

Task 1 (Software Simulation Tools)

(1B): Develop software design tools that fully account for multiple scattering within the holographic Bragg reflector structure.

Task 4 (Device Wafer 1: 4-channel mux)

(4A) Utilizing previously developed software (modified in accordance with previously obtained test results), design a set of four-channel planar holographic HBR multiplexer devices. Design for optimal spectral transfer function profile. In various specific designs, test approaches to apodization and holographic overlay.

(4B) Fabricate Device Wafer 1

(4C) Test and characterize the various designs of Device Wafer 1. Compare measurements with predicted performance and analyze to improve and refine design algorithms.

Task 5 (Design and Fabricate Device Wafer 2 – Minimal insertion loss devices)

(5A) Utilize advanced design algorithm and previously developed software to design a set of planar holographic multiplexers including devices with > 4 spectral channels. Design for high reflectivity (<1 dB device insertion loss). Optimize spectral transfer function to nearly flat top with rapid cut-off at the edges of the desired bandpass window (approx 40 GHz) and locate on adjacent channels on the ITU grid.

Accomplished Technical Activities and Development, Summary of Results

The third reporting period of the present Phase II SBIR project has been completed successfully.

In test results of previous fabrication runs we had identified certain discrepancies between measured and design multiplexer spectral transfer functions and attributed those to a second-order coupling between the grating amplitude apodization method employed to the effective waveguide index. In the present reporting interval we have successfully

modeled this effect. The agreement between data and simulated performance is now close to perfect. This indicates that (1) the fabrication has rendered the actual designs with excellent fidelity and (2) that the effect is well-understood and consequently appropriate provisions in the design algorithm of future iterations will mitigate it. Additionally, LightSmyth is presently developing alternative amplitude apodization methods that largely decouple the reflective amplitude from the reflective phase.

Furthermore, a model to evaluate the reflective bandwidth of planar slab waveguide-based volume-holographic structures has been developed and has been applied to the present device architecture to evaluate the number of DWDM channels supported. A new highly reflecting device geometry has been developed and was evaluated through testing to provide DWDM channel multiplexer numbers in excess of that required for complete coverage of the ITU C-band.

Additionally, we have identified and tested (by comparison to test results) a simulation and design tool that will allow to evaluate the performance of distributed Bragg structures in the limit of high reflectivity where multiple scattering and input beam depletion has to be accounted for.

Summary of Results and Accomplishments
Reporting period 2/1/2005 - 7/31/2005

- Successfully modeled second-order amplitude apodization effect
- Excellent agreement between improved simulation and measurement attests to high-fidelity DUV fabrication
- Future mitigation via compensation incorporated in design algorithm
- Alternate apodization methods decouple reflective amplitude and phase – presently under development
- Developed model to predict reflective band width of previous and alternate waveguide architectures
- Fabricated new dual-core waveguide grating structure demonstrates reflective bandwidth enabling multiplexer operation in excess of ITU C-band
- Identified and evaluated simulation tool for modeling of HBR structures in high-reflectivity regime

2. Status Report

2.1. Milestones/Task Status

2.1.a. Project Status

The project is presently on schedule. An updated task table outlining the status of tasks pertinent to this reporting period is given below.

Updated Task Schedule

<table>
<tr><th>Month</th><th>Task 1</th><th>Task 2</th><th>Task 3</th><th>Task 4</th><th>Task 5</th><th>Task 6</th></tr>
<tr><td>1</td><td rowspan="8">(1A) Develop 2D Fresnel Sim using Weak Scattering Approx COMPLET-ED</td><td rowspan="4">(2A-2C) Test & Fab Standards Wafer COMPLET-ED</td><td></td><td></td><td></td><td></td></tr>
<tr><td>2</td><td></td><td></td><td></td><td></td></tr>
<tr><td>3</td><td></td><td></td><td></td><td></td></tr>
<tr><td>4</td><td></td><td></td><td></td><td></td></tr>
<tr><td>5</td><td rowspan="4">(2D) Birefring-ence Mitigation COMPLET-ED</td><td></td><td></td><td></td><td></td></tr>
<tr><td>6</td><td></td><td></td><td></td><td></td></tr>
<tr><td>7</td><td rowspan="6">(3A) Test Designs (3B) Fab Prelim DeviceWafer (3C) Test and Refine (1A) COMPLET-ED</td><td></td><td></td><td></td></tr>
<tr><td>8</td><td></td><td></td><td></td></tr>
<tr><td>9</td><td rowspan="16">(1B) Develop Strong Scattering Sim

IN PROGRESS</td><td></td><td></td><td></td><td></td></tr>
<tr><td>10</td><td></td><td></td><td></td><td></td></tr>
<tr><td>11</td><td></td><td></td><td></td><td></td></tr>
<tr><td>12</td><td></td><td></td><td></td><td></td></tr>
<tr><td>13</td><td></td><td></td><td rowspan="5">(4A-4C) Design, Fab, & Test Dev. Wafer 1 4-channel mux COMPLET-ED</td><td></td><td></td></tr>
<tr><td>14</td><td></td><td></td><td></td><td></td></tr>
<tr><td>15</td><td></td><td></td><td></td><td></td></tr>
<tr><td>16</td><td></td><td></td><td></td><td></td></tr>
<tr><td>17</td><td></td><td></td><td rowspan="7">(5A-5D) Design, Fab, & Test Dev. Wafer 2 4,8,16-channel mux Low Ins. Loss IN PROGRESS</td><td></td></tr>
<tr><td>18</td><td></td><td></td><td></td><td></td></tr>
<tr><td>19</td><td></td><td></td><td></td><td></td></tr>
<tr><td>20</td><td></td><td></td><td></td><td></td></tr>
<tr><td>21</td><td></td><td></td><td></td><td rowspan="4">(6A-6C) Document & Evaluate</td></tr>
<tr><td>22</td><td></td><td></td><td></td></tr>
<tr><td>23</td><td></td><td></td><td></td><td></td></tr>
<tr><td>24</td><td></td><td></td><td></td><td></td><td></td></tr>
</table>

2.1.b. Comparison of Achieved End-Product Performance

Not applicable.

2.1.c. Description of Technical Developments and Accomplishments including Effort Expended on Each Task to Date

Task 1B: Development of Software Simulation Tools. Time expended during the reporting period (February 1, 2005 through July 31, 2005) for this effort was 269 hours.

We have investigated several simulation methods, commercially available as well as ones reported in the literature, that fully account for multiple scattering within distributed Bragg structures. This problem is mathematically similar to the problem faced in simulating the performance of highly reflective fiber Bragg gratings. Since fiber Bragg gratings have been under development for several years now precise commercial design and simulation tools are available from multiple vendors. Typically, these tools are based on coupled-mode theory and simulate only one-dimensional periodic index variations. Since the planar holographic devices under present development operate primarily in the paraxial regime (very close to retro reflection and thus essentially fiber-Bragg-grating-like one-dimensional operation) we expected these commercial tools to provide sufficient guidance with respect to HBR spectral transfer simulation. During the last reporting interval, we have compared multiple simulation results obtained with one coupled-mode package, OptiWave's OptiGrating, to our experimental measurements and found that the agreement between data and simulation has been quite excellent and that the package thus provides a great design and diagnostic tool.

Task 4: 4-channel DWDM mux fabrication, testing and performance analysis. Time expended during the reporting period (February 1, 2005 through July 31, 2005) this task was 360 hours.

In the previous reporting interval we had designed, fabricated and done preliminary testing on several HBR-based multiplexing devices for dense wavelength division multiplexing. Our results successfully demonstrated wavelength division multiplexing based on holographic Bragg reflectors, tested tailoring of spectral transfer function design using the partial writing and offsetting of diffractive contours and demonstrated the use of overlaid planar holograms to design compact-foot print multiplexers.

In these previous test results spectral transfer functions occasionally exhibited small discrepancies when compared to designed spectral transfer functions. We hypothesized that the origin of this behavior is a coupling between the partial writing of contours employed for amplitude apodization and the effective waveguide index. In the present reporting interval we have quantitatively investigated this effect and incorporated it in our simulation tools. The agreement between improved simulation results and data is now near-perfect indicating that the photolithographic fabrication process has reproduced the designs with great fidelity. Since the coupling between amplitude apodization and effective waveguide index is now fully quantified it can be included in the design software for future iterations. Other pathways to device apodization are also presently under investigation at LightSmyth. We describe our results in detail in the following.

To illustrate the aforementioned apodization effect we show in Figure 1 design, measurement and improved simulation results for an individual channel of an HBR-based multiplexer. An amplitude-only adpodization profile consisting of a Gaussian-weighted cosine based on the partial-fill method was used to create the spectral transfer function shown in Figure 1a. Note the improved suppression (> 20dB) of sidelobes immediately

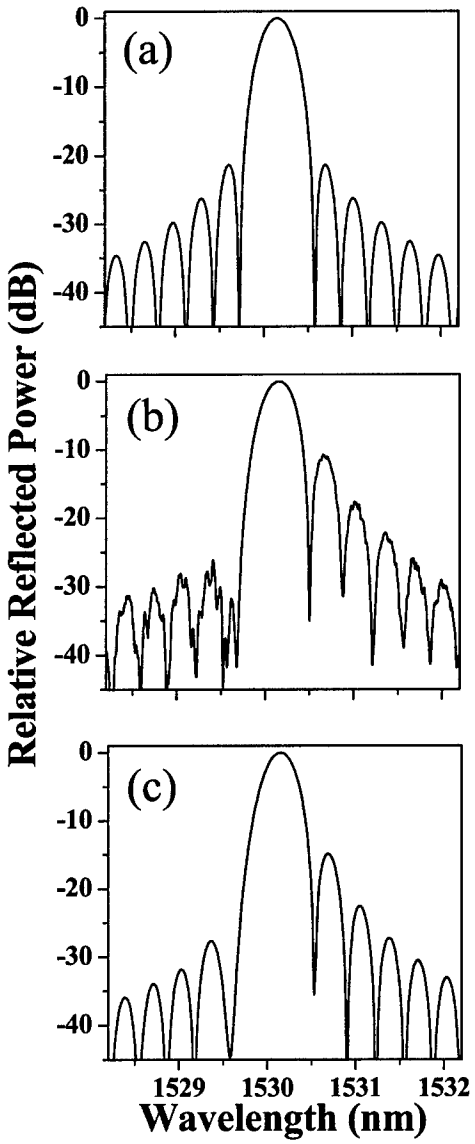

Figure 1. Detail of the passband function for an individual HBR multiplexer channel. 1a, Simulated throughput, calculated with constant effective index. 1b, Measured throughput (for TE-polarization). 1c, Simulated throughput, calculated with account for apodization-induced effective index changes.

adjacent to the main channel passband compared to that typically observed (~ 13dB) in an unapodized grating device. Figure 1b gives the measured spectral transfer function of the channels of the fabricated device for TE-polarized input light. Agreement between

measured and designed performance is good except for the unexpectedly high side lobes on the long wavelength side of each primary passband.

The long-wavelength sidelobes in the measured multiplexer response illustrate the aforementioned second-order apodization effect, detailed below, that was unaccounted for in the device designs. The second-order effect comprises an effective refractive index variation inadvertently introduced by using partial contour fill to effect amplitude apodization. In the previous multiplexer designs, apodization of the reflective amplitude of HBR diffractive contours was achieved through partial contour writing. Nominally continuous diffractive contours are written fractionally, with the written contour fraction determining the contour's reflective amplitude. Contour writing occurs through etching (and filling with cladding material) of trenches into the core. Variations in the written trench fraction due to amplitude apodization lead to differences in waveguide morphology that cause variations in the slab waveguide effective refractive index and consequently the Bragg resonance condition.

We have performed measurements on various test grating structures, each having diffractive contours of fixed written fraction, show a small and approximately linear variation of effective waveguide refractive index with written trench fraction. Specifically, for a slab waveguide core of thickness d = 4 μm and 450 nm deep diffractive trenches (as used in the previous multiplexer architecture) the effective waveguide index was measured to vary as

$$n_{eff}(r) = n_o(1 - 2\times10^{-4} G(r)),$$

where n_o is the effective index of the slab waveguide in the absence of the HBR contours and $G(r)$ is the written diffractive contour fraction at position r.

In Figure 1c we explore the impact of the apodization-induced resonance shifts on the multiplexer spectral transfer function. The figure shows the passband profile simulated including the effect of the measured apodization-induced effective refractive index changes. A comparison of Figures 1b (measurement) and 1c (improved simulation) shows that the simulation now clearly reproduces all features of the fabricated device. The near-perfect agreement between data and improved simulation attests to the precision fabrication capability of the DUV-photolithographic approach.

We have also incorporated the second-order apodization effect in the performance simulation of the previously fabricated 4-channel 100-GHz-channel-spacing flat-top-passband HBR multiplexer. The device was described in detail in the previous status report. The device comprises apodized individual-channel HBRs that are staggered along the input beam direction but are also heavily overlapping. For reference, we show in Figure 2a (2b) the design (measured) spectral transfer functions of the various multiplexer channels for TE-polarized input light. Measured passbands clearly exhibit the designed flat passband and channel spacing as well as excellent adjacent channel isolation of >-22 dB.

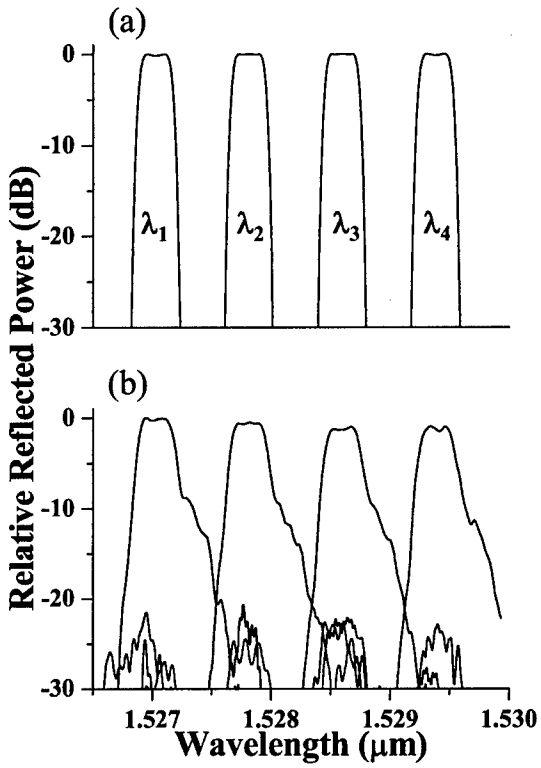

Figure 2. Spectral transfer function of multiplexer based on overlaid HBRs. 2a, Design (constant effective index). 2b, Measured multiplexer spectral transfer function (for TE-polarization).

Discrepancies between measured and designed channel transfer functions such as the long-wavelength shoulder of the measurement are observed. Two principally different factors are causing these. The first is the aforementioned apodization-induced effective index change that is not compensated for in the present multiplexer design. Additionally, the various individual-channel holograms were overlaid without taking detailed precaution to avoid overlap of diffractive contours belonging to different holograms. Because of this, when portions of a given hologram coincide with diffractive contours of a different grating they exhibit a reflective amplitude that is reduced from its design value. To summarize, the actual hologram apodization is altered from the original design value through two position-dependent effects, i.e. (1) variations in slab waveguide effective refractive index and (2) variations in expected reflective amplitude. Both effects must be accounted for to correctly predict the bandpass function of the fabricated multiplexers.

Figure 3 explores the impact of the above described phenomena on the spectral transfer function of the λ_1 multiplexer channel. Figure 3a is a blow up of the original design passband function calculated with constant effective index and without account for the reduction of reflective amplitude caused by hologram overlap. Figure 3b shows the detailed measured TE-polarized spectral response for the same channel. Figure 3c shows the passband profile simulated with both the spatially varying effective refractive index and reflective amplitude changes accounted for as described below.

The apodization and overlap effects lead to a position-dependent effective waveguide refractive index which we have modeled (guided by test results on auxiliary structures) as

$$n_{eff}(r) = n_o(1 - 6 \times 10^{-4}(1 - R(r)),$$

where *R(r)* is the unetched (no written trenches) fraction of slab waveguide at each position, *r*, within the device and n_o is the effective index of the slab waveguide in the absence the HBR contours. *R(r)* was calculated according to

$$R(r) = \prod_{i=1}^{N} (1 - \alpha_i \times G_i(r)),$$

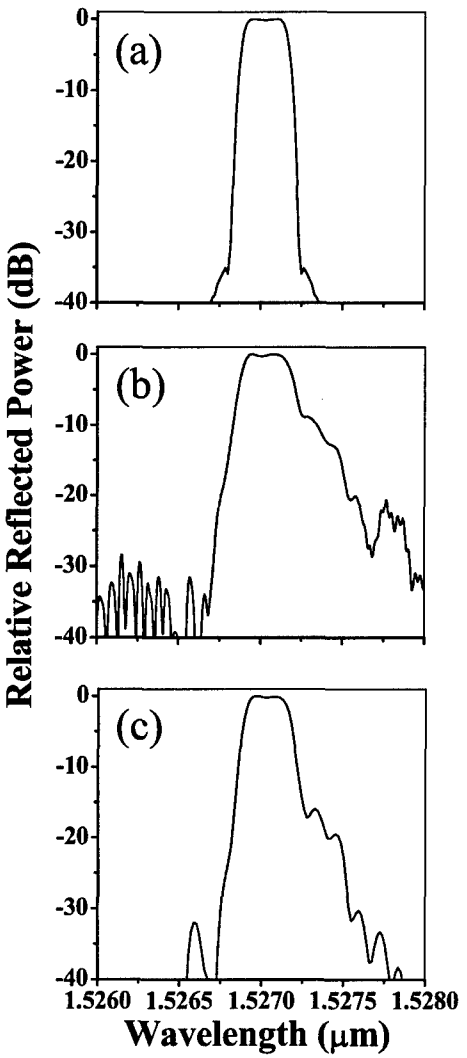

Figure 3. Blow-up of an multiplexer channel. 3a, Constant effective index simulation. 3b, Measured passband. 3c, Multiplexer throughput calculated including apodization-induced effective index variations and reflective amplitude reduction due to hologram overlay.

where $G_i(r)$ is the written diffractive contour fraction of the ith planar grating at position r and α_i is its duty cycle. The summation runs over all HBRs written. In the present multiplexer design all gratings operate in the first grating order, thus $\alpha_i = 0.5$ for i = 1,..., N.

The reflective amplitude of the j^{th} planar hologram as modified by grating superimposition is written as

$$A_j(r) = A_j'(r) \prod_{i=1, i\neq j}^{N} (1 - \alpha_i \times G_i(r)),$$

where $A_j'(r)$ is the apodization function that pertains in the absence of overlap. The product runs over all HBRs except for the j^{th}. As comparison of Figures 3b and 3c shows, the simulation now clearly reproduces all features of the fabricated device. The agreement between the simulation of Fig. 3c and the measured bandpass spectrum of Fig. 3b is quite excellent. It is apparent from this agreement that the photolithographic fabrication method employed reproduced the design set of grating elements with great precision.

In future design iterations multiplexer designs will be simply corrected for the effect of apodization-induced effective refractive index changes by scaling the separation between grating lines to keep optical path distances at appropriate values. The reduction of reflective amplitude caused by overlay of multiple holograms may be avoided by employing higher grating orders or lower peak fill fractions and implementing a design algorithm wherein spatially overlapping contour elements are displaced to avoid overlap. Alternatively, overlap effects can be incorporated into the apodization design algorithm. Additionally, alternate methods to amplitude apodization that decouple reflective phase and amplitude to a large degree are presently underway at LightSmyth. We will report on these and test results in the next reporting interval.

Results

- Successfully modeled second-order amplitude apodization effect
- Excellent agreement between improved simulation and measurement attests to high-fidelity DUV fabrication
- Future mitigation via compensation incorporated in design algorithmn
- Alternate apodization methods decouple reflective amplitude and phase – presently under development

Task 5A (Design Device Wafer 2 – Minimal insertion loss devices) Time expended during the reporting period (February 1, 2005 through July 31, 2005) this task was 209 hours.

The previously fabricated HBR multiplexers were proof-of-principle devices realized in a low-index contrast waveguide architecture. The choice of the latter was motivated by our desire to be compliant with a proven standard fabrication process. To succeed at fabricating a competitive HBR-based multiplexer it is necessary to estimate what reflective bandwidth (and specifically what number of DWDM channels) the present geometry and alternate waveguide architectures can support while maintaining minimal insertion loss. To this end, we have developed a model in this reporting interval, that allows us to estimate the number of DWDM channels supported by a given waveguide geometry. The model will give guidance with respect to the optimal waveguide geometry to be used in the next fabrication run. We detail this model and our channel number evaluation in the following.

HBR devices are reflective in nature. More specifically, they depend on cooperative reflection from distributed arrays of diffractive elements (contours) each of which is by itself a weak scatterer. There are fundamental constraints that connect the total number, N, of diffractive elements in an HBR (or alternatively the length, L, of the HBR), the diffractive scattering amplitude of each element, r_a, the total spectral bandwidth over which the device is to reflect, $\Delta\nu_t$, and the required reflective strength. Dense WDM devices (e. g. a 16-channel multiplexer) require high reflectivity over an aggregate bandwidth that can be approaching tens of nanometers.

We wish to estimate the spectral bandwidth (which may or may not be contiguous) over which a first-order HBR of constrained length L and simple internal geometry can provide high reflectivity. Consider the quarter-wave reflective stack shown in Figure 4a. The stack consists of planar interfaces between materials of refractive index n_1 and n_2. Let $\Delta n = |n_2 - n_1|$ and $n = (n_1 + n_2)/2$. The planar interfaces are spaced by $\Lambda/2$ and produce strong Bragg backscattering at vacuum wavelength $\lambda_B = 2n\Lambda$. The incident wave (assumed incident normal to the interfaces) is attenuated and exhibits a 1/e penetration depth of approximately $d = n\Lambda/q\Delta n$. For the quarter-wave stack, $q = 1$. The corrugated slab waveguide of Figure 4b exhibits similar behavior except that the factor q, defined as the ratio of back scattered field amplitudes produced by the corrugation and plane interfaces, is less than one. A regular diffractive structure of length d has a weak-signal Fourier-transform spectral bandpass of approximately $\Delta\nu_d \approx c/4nd$, where c is the vacuum light speed. We use this bandwidth to approximate that of diffractive structures of 1/e-field penetration. In the following, we assume that an HBR of length $L > d$ may be viewed as a number of segments of length, d, each of which has bandwidth $\Delta\nu_d$ and operates at 1/e field transmission. To achieve a broad reflection band, the various HBR segments are chirped or frequency shifted. The construction described is consistent with an overall HBR reflection bandwidth $\Delta\nu_{tot}$ given by

$$\Delta\nu_{tot} = \frac{L}{d}\Delta\nu_d = \frac{cL\Delta n^2 q^2}{4\Lambda^2 n^3}$$

Figure 4c depicts the electric field mode of a corrugated slab waveguide modeled after our fabricated structure. Calculating the field area under the corrugated region and

dividing by the total field area, we determine $q \approx 0.06$. With $L = 1$ cm, $\Lambda = 0.5$ μm, $n \approx 1.45$, for the slab waveguide geometry with 0.8 % index contrast shown in Figure 4c,

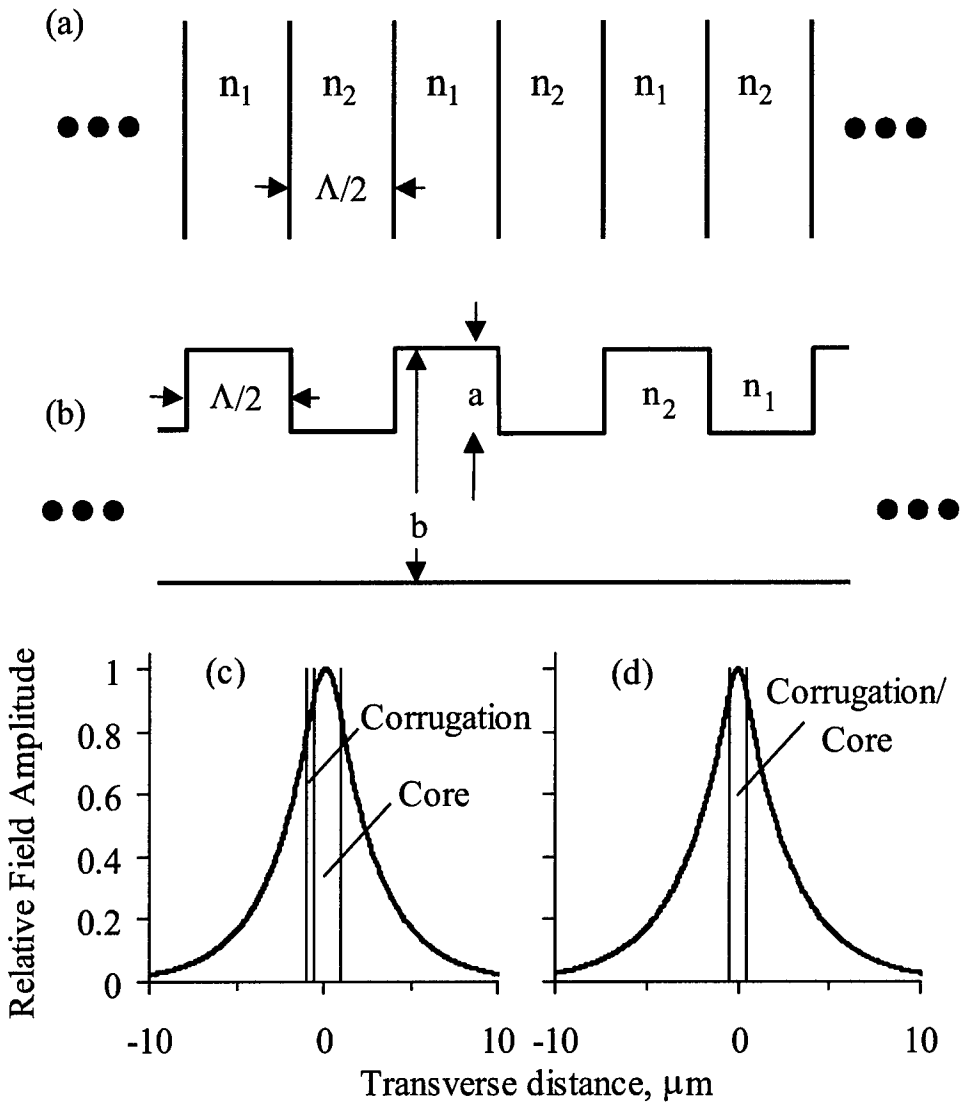

Figure 4. (a) Quarter-wave stack of planar interfacial reflectors. (b) Corrugated planar waveguide reflector model of HBR. (c) Plot of modal electric field for the corrugated slab waveguide configuration fabricated and tested (0.4 μm corrugation etched in 2 μm thick waveguide). (d) Plot of the modal electric field for a very broad reflection bandpass slab waveguide structure (see text).

we get $\Delta\nu_{tot} \approx 4\times10^{11}$ Hz which corresponds to about a 3-nm reflective bandwidth or about 6-7 DWDM channels at the operative wavelength.

We shift our attention to predicting how one might produce an HBR capable of reflecting over several tens of nanometers as needed for general DWDM mux applications. In Figure 4d, we show the modal electric field for a 1-μm-thick slab waveguide whose corrugations extend entirely through the slab (a = b in Figure 4b). The value of Δn has been increased by a factor of three to approximately 0.03. The q-factor is

Results

- Developed model to predict reflective band width of previous and alternate waveguide architectures
- Fabricated new dual-core waveguide grating structure demonstrating reflective bandwidth enabling multiplexer operation in excess of ITU C-band

found to be 0.16. With these parameters, we find that $\Delta\nu_{tot} \approx 3\times10^{+13}$ Hz, which corresponds to about a 210-nm reflective bandwidth at the operative wavelength – broad enough to support a multiplexer channel number exceeding the ITU C-band. It should be noted the etch aspect ratio needed to produce the described broadband HBR device has been demonstrated as part of the LightSmyth development program.

An additional consideration with respect to the overall device insertion loss is the fiber-to-waveguide coupling loss. The modal structure of the planar waveguide has to be matched properly to that of the incoupling single-mode fiber to avoid excess losses. We have developed a new high-reflectivity waveguide architecture that addresses this issue and optimizes the fiber-to-waveguide-coupling. Figure 5, left side, is a cross-sectional view of a recently optimized dual core layer geometry. The right side shows the reflection spectrum of a simple uniform 900-μm-long HBR test structure with a 3.3-nm 3-dB bandwidth. Modeling results indicate that, for the given HBR length, this reflective band width corresponds to an extinction length of 270 μm. Using the previously derived formula for the overall available reflective bandwidth we find $\Delta\nu_{tot}$ to be ~100 nm in a HBR-structure of 1 cm length for the new device geometry – enough to support in DWDM channel numbers in excess of the C-band, while at the same time providing more optimal fiber-to-waveguide coupling than the geometry shown in Figure 4c.

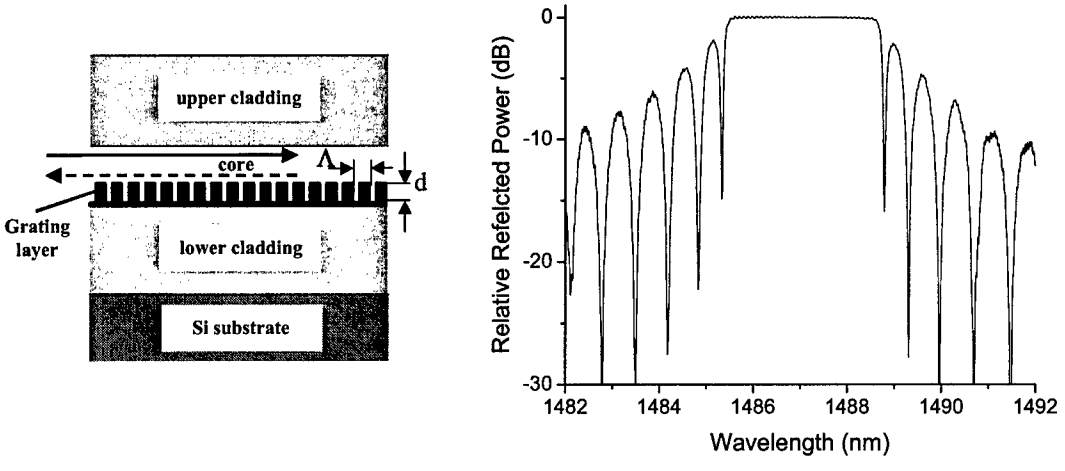

Figure 5. Left, Cross-sectional view of new high reflectivity waveguide architecture based on dual-layer core. The 500-nm thick high index grating layer has a 2 % index contrast with respect to the upper core layer. Right, measured reflection spectrum for 900-μm-long HBR test structure exhibiting a 3.3-nm bandwidth. The corresponding extinction length is 270 μm.

2.1.d. Testing: Key Dates, Tests Performed and Results

Results of device tests were described in detail in section 2.1.c..

2.1.e. Compilation and Description of Completed Designs

A detailed description of the test and device structures designed in this 6-month effort is given in section 2.1.c..

2.1.f. Resolution Status of Outstanding Problems Identified in Previous Report

Not applicable.

2.1.g. Problems Encountered or Anticipated

No problems were encountered in the period this document reports on nor are any presently anticipated.

2.1.h. Results of Conferences, Trips or Directives from Contracting Officer's Representatives

Following is a list of conference presentations given during the reporting interval on LightSmyth development of the holographic Bragg reflector technology:

1. T. W. Mossberg, C. M. Greiner, D. Iazikov, "Submicron planar waveguide diffractive photonics (Invited Paper)", Conference on Integrated Optics: Devices, Materials, and Technologies IX, Photonics West, 22–27 January 2005, San Jose, California, USA.

2. C. M. Greiner, T. W. Mossberg, D. Iazikov, "Planar lithographic holography as enabler of integrated photonics (Invited Paper)", Conference on Practical Holography XIX: Materials and Applications, Photonics West, 22–27 January 2005, San Jose, California, USA.

3. C. M. Greiner, D. Iazikov, T. W. Mossberg, " Fully-Integrated Planar-Waveguide Resonator Optics Based on Holographic Bragg Reflectors," in *Optical Fiber Communication Conference and Exposition and The National Fiber Optic Engineers Conference on CD-ROM* (Optical Society of America, Washington, DC, 2005), OFK5.

4. T. W. Mossberg, D. Iazikov, and C. M. Greiner, "Amplitude apodization in lithographically-scribed planar waveguide holograms via correlated line set displacement," in *Integrated Photonics Research and Applications/Nanophotonics for Information Systems Topical Meetings on CD-ROM* (The Optical Society of America, Washington, DC, 2005), IMB6.

5. C. Greiner, D. Iazikov, and T. W. Mossberg, "Fully-Integrated Planar-Waveguide Resonator Optics Based on Holographic Bragg Reflectors," in *Integrated Photonics*

Research and Applications/Nanophotonics for Information Systems Topical Meetings on CD-ROM (The Optical Society of America, Washington, DC, 2005), ITuC6.

2.1.i. Other Information concerning Program Schedule Changes

N/A.

2.2. Future Plans

Plans for the immediate future comprise completion of tasks as outlined in the updated work plan of section 2.1.a. and described in-depth by task number in the original proposal on pages 29 – 34.

2.3. Itemized Man-Hours and Costs

Month	Man-Hours	Costs
February 2005	132.0	$25,385.84
March 2005	167.5	$32,213.10
April 2005	135.5	$26,058.95
May 2005	135.0	$25,962.80
June 2005	159.0	$30,578.40
July 2005	109.0	$20,962.55
Total for Reporting Period	838.0	$161,161.64

2.4. Contract Deliveries Status

Contract Line Item No. 0002, for Data Item No. A002, initial Status Report was delivered as per the requirements of the contract data requirements list (CDRL). Subsequent Status Reports to be submitted after the completion of 12 month's work and 18 month's work. Final Technical Report to be submitted at the conclusion of the project as per Contract Line Item No. 0002 and Data Item No. A001.

2.5. Report Preparer

Dr. Christoph M. Greiner, Senior Scientist, LightSmyth Technologies
Tel.: 1-541-431-0029, E-mail: cgreiner@lightsmyth.com

3. Appendices

None.